



Optimisation of the removal of arsenate from water using nanochitosan

Anand Sreeram^a, Pejman Hadi^a, Chi-Wai Hui^a, Tareq Al Ansari^b, Gordon McKay^{b,*}

^aDepartment of Chemical and Biomolecular Engineering, Hong Kong University of Science and Technology Clear Water Bay, Kowloon, Hong Kong SAR, China, emails: 78anand@gmail.com (A. Sreeram), kehadi@ust.hk (P. Hadi), kehui@ust.hk (C.-W. Hui)

^bDivision of Sustainability, College of Science and Engineering, Hamad Bin Khalifa University, Education City, Qatar Foundation, Doha, Qatar, email: gmckay@qf.org.qa

Received 15 October 2016; Accepted 14 January 2017

ABSTRACT

In this study, the removal of arsenate from water using a nanochitosan adsorbent is investigated, and an optimised two-stage batch adsorber system is designed. Nanochitosan is a widely researched biosorbent that is derived from seafood shell waste. An equilibrium study was first conducted with a contact time to reach equilibrium of 3 d. These results were used to minimise the mass of chitosan required in a two-stage batch adsorption process using an optimised design procedure. Subsequently, the adsorption kinetics were modelled, and a contact time study was conducted to acquire the time required using a pseudo-second-order model. The mass and contact time required in an optimised batch adsorber system was found to be around 1–3 kg, depending on initial arsenate concentration, and close to 100 min, respectively.

Keywords: Arsenate removal; Nanochitosan; Batch adsorption optimisation

1. Introduction

Arsenic (As) is a commonly found element that is present in the atmosphere, soil, organisms, and natural waters. Arsenic is found in nature as either metalloids or chemical compounds and mainly exists as two principal species: arsenate and arsenite. Arsenic contamination in natural waters is a global problem and has been reported in many countries around the world. Arsenic has been known for its hazardous effect on both flora and fauna ever since it was first documented by Albertus Magnus in 1250 AD [1]. The main path of arsenic transportation into the environment and biological systems is the consumption of arsenic contaminated water. Arsenic in aqueous environments mainly exists in the 3⁺ (As(III), arsenite) and 5⁺ (As(V), arsenate) oxidation states although other oxidation states such as 0 (arsenic) and 3⁻ (arsine) are also known to exist [2]. Arsenate and arsenite species are the dominant forms of arsenic that are generally detected in groundwater and are more toxic than organic arsenic species such as

methylated arsenic. It has been previously observed that the ratio of As³⁺ to As⁵⁺ in groundwater is unstable due to the availability of redox active solids, mainly organic carbon and the extent of diffusion of oxygen from the atmosphere, although arsenate is the most common form, which is found in nature [3]. The instances of arsenic poisoning through water have been well documented. In 1898, the first cases of skin cancer were observed among the population consuming arsenic contaminated water in Poland. The deep well contamination of arsenic in the rocky mountain areas of Ontario, Canada, in the year 1937 was one of the first known cases in North America. In Asia, the arsenic contamination incident in well water on the southwest coast of Taiwan during the period from 1961 to 1985 is well known. During the 1980s, the endemic arsenicosis was found in several areas of Mainland China including Xinjiang Uygur A.R., Inner Mongolia, Shanxi, Liaoning, Jilin, Ningxia, Qinghai and Henan provinces [4]. The decontamination and reduction of arsenic elements from water supplies is always a priority for scientists as the admissible levels, and concentration limit decreases continuously based on health criteria in waters. Table 1 summarises the maximum contaminant level of arsenic in different regions of the world.

* Corresponding author.

The main treatment methods used for the removal of arsenic from groundwater are based on the principles of co-precipitation [11], adsorption, ion exchange, electrocoagulation and filtration [12–17]. Adsorption is one of the most commonly used technologies for wastewater treatment offering low costs, simple operability and relatively high efficiency. Specifically, the treatment of arsenic using adsorption has been popular over the past years. Arsenic chemistry is very similar to phosphorous chemistry, and its selective adsorption utilising biological materials, mineral oxides, activated carbons, polymer resins and most recently graphene has been widely researched [18–23]. A wide range of adsorbents such as bone char, MCM-41, coconut shell carbon and chitosan has been reported in the past for removing arsenic species removal from water [24–27]. Table 2 shows the biosorption capacities of several adsorbents for arsenate.

This study is concerned with a design and optimisation of a two-stage batch operating system for the removal of arsenate species from wastewater using nanochitosan. Chitosan is a nitrogenous polysaccharide, which is produced by the N-deacetylation of its origin compound chitin, one of the most abundant biopolymers, and exists in marine media, also in the exoskeletons of crustaceans or cartilages of molluscs, cuticles of insects and cell walls of organisms. Chitosan has been shown to have a wide range of applicability across different industries including biotechnology, pharmaceutical applications, wastewater treatment for oil spills and coloured effluents [36–42]. Additionally, as a result of its molecular structure, chitosan has an extremely high affinity for many classes of metals, dyes and

surfactants [43–46]. The potential to develop nanoparticles using chitosan is high because of its ability to control the release of the active agents, its linear polyamine structure containing numerous free amine groups for cross links and its mucoadhesive character for increasing the residence time at the adsorption site. The mechanism of arsenic removal using chitosan and nanochitosan has been studied by a number of researchers [29,47,48] but the application to process design is severely lacking.

2. Experimental procedure

2.1. Materials

2.1.1. Preparation of nanochitosan emulsions

Commercial chitosan was sieved into discrete particle size ranges (250–355, 355–500, 500–710 and 710–1,000 μm) with test stainless steel sieves (BS410/1986, Endecotts Ltd., London, UK). The portions were dried under vacuum for 3 d and kept in a desiccator before use. Firstly, 2.5 g raw material of chitosan (powder form) was completely dissolved in 1% (w/v) dilute acetic acid under magnetic stirring, and the emulsion was prepared as reported previously [49]. Typically, a tripolyphosphate (TPP) solution (95.4 mL, 1.45 mg/mL) was slowly dropped (10 mL/min) into a chitosan solution (150 mL, 2 mg/mL in 0.5% dilute acetic acid) in a 500-mL round-bottom flask under mechanical stirring (1,200 rpm/min). After a further stirring of 20 min, a milky emulsion was obtained at pH 5.0. The nanoparticles were obtained by freezing the emulsion at -4°C . The frozen emulsion was then thawed in the atmosphere, and the nanoparticles were precipitated [50]. After another stirring for 24 h, the nanoparticles were collected after a centrifugation for 24 h. They were then washed with deionised water and vacuum dried at 60°C for 24 h. After vacuum drying the particle size range of the nanochitosan was 150–250 nm using a zetasizer (Malvern).

2.1.2. Factors affecting equilibrium contact time

The time to reach equilibrium was found to be 3 d. Further series of experiments using different initial pH values from 3 to 5 indicated that the optimum uptake capacity occurred with an initial pH of 3.5. On this basis, all equilibrium studies in the present work would use a contact time of 4 d to ensure equilibrium has been achieved over the whole concentration spectrum and used an initial pH of 3.5.

2.1.3. Experimental equilibrium studies

To determine the equilibrium isotherms, a series of As(V) solutions with initial concentrations ranging between 250 and 10,000 $\mu\text{g/L}$ were prepared by diluting a 500-mg/L stock solution with deionised water. The pH and temperature values were maintained at $3.50^{\circ}\text{C} \pm 0.05^{\circ}\text{C}$ and at $24^{\circ}\text{C} \pm 2^{\circ}\text{C}$, respectively. Subsequently, 0.0250 g of nanochitosan was agitated with 50 mL of aqueous As(V) solution in capped 125-mL HDPE bottles with an orbital shaker at 200 rpm for 96 h. This contact time allows the dispersion of adsorbent and arsenate solution to reach equilibrium, as determined during preliminary experiments. Each tested suspension was collected after sufficient settling time of 2 min, and then the upper clear solution was collected for measuring of residual As(V) concentration.

Table 1
Worldwide drinking water standard for arsenic in water

Country	Drinking water standard ($\mu\text{g L}^{-1}$)	Reference
World Health Organization	10	[5]
Australia	7	[6]
China	50	[4]
European Union	10	[7]
India	50	[8]
Taiwan	10	[9]
US	10	[10]

Table 2
Biosorbent uptake capacities of arsenate in water

Biosorbent	pH	Biosorption Capacity (mg/g)	Reference
Canna indica	4	0.487	[28]
Chitosan	4	96.46	[29]
Cotton cellulose	5	75.13	[30]
Eggshell	7.2	2.82	[31]
Pine saw dust	4	12.85	[32]
Rice husk	6	27.83	[33]
Waste crab	4	35.92	[34]
Wheat straw	3	3.90	[35]

2.1.4. Experimental sorption kinetic studies

The sorption kinetic studies of As(V) on nanochitosan were evaluated by agitating 0.850 g of sample in 1.7 L of aqueous As(V) solution for 6 h in a batch kinetic system, shown in Fig. 1. The impeller speed was calibrated to 400 rpm; the temperature and pH were maintained at $24^{\circ}\text{C} \pm 2^{\circ}\text{C}$ and 3.50 ± 0.05 , respectively. The pH of the As(V) solution with a predetermined concentration of arsenate was adjusted to the range from 3.50 to 0.05. This ensures that the solution remains at an acidic pH throughout the adsorption process keeping the chitosan protonated to attract the negative arsenate species. The relative dimensions of the sorber vessel are also presented in Fig. 1. Arsenate concentrations ranging from 1,000 $\mu\text{g/L}$ to 10,000 $\mu\text{g/L}$ were employed, and agitation was carried out for 6 h until over 70% equilibrium was attained. Constant agitation was achieved using a six-bladed Perspex impeller and a shaft driven by a Heidolph variable speed motor. Since several adsorption studies were performed in parallel, the agitation conditions must be constant in all systems in case there is a boundary layer external mass transfer effect, which must be maintained the same in all the systems.

2.1.5. Analysis of arsenate

All chemicals were reagent grade and were used without further purification. All solutions were prepared with deionised water, and all laboratory ware was cleaned by soaking in 2% diluted nitric acid (HNO_3) and rinsed with deionised water. A stock solution of As(V) was prepared from the dissolution of sodium arsenate heptahydrate salt ($\text{Na}_2\text{HAsO}_4 \cdot 7\text{H}_2\text{O}$) at a concentration of 500 mg/L. Hydride generation inductively coupled argon plasma optical emission spectroscopic analysis using a continuous flow system (Perkin Elmer OPTIMA 3000 XL) was used to measure the concentration of arsenate in water. All experiments were done in triplicate and the average error was $\pm 6\%$.

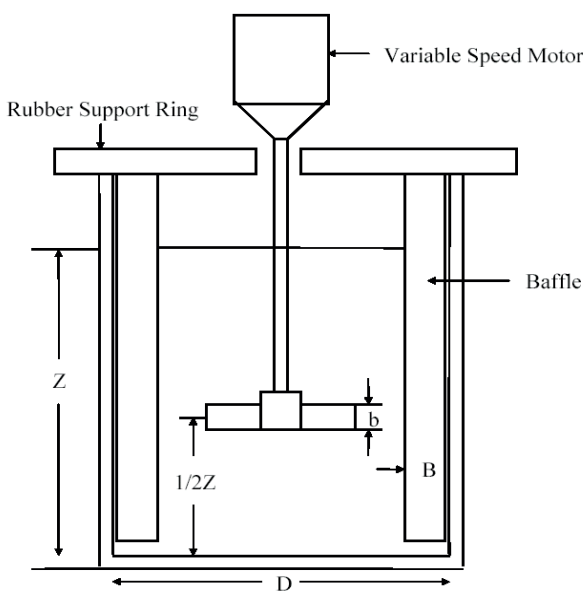


Fig. 1. The schematic diagram of batch stirred-tank.

3. Results and discussion

3.1. Equilibrium isotherms

To determine the adsorption capacity of arsenic on nanochitosan and for process design purposes, equilibrium adsorption data is required. The equilibrium models are generally formulated around kinetic considerations, wherein adsorption equilibrium is defined as being a state of dynamic equilibrium with both adsorption and desorption rate equal [51]. Different isothermal models were tested to determine the isotherm constants and the regression coefficients of the adsorption experimental results including the Langmuir model, the Freundlich model, the Sips model, the Redlich–Peterson model, Temkin model and the Toth model. The results of the equilibrium modelling are shown in Fig. 2.

3.1.1. Langmuir isotherm

The Langmuir adsorption model was developed for describing the gas–solid phase adsorption onto an activated carbon after which it has been traditionally used to quantify and contrast the performance of different adsorbents [52]. It is represented by Eq. (1):

$$q_e = \frac{K_L C_e}{1 + a_L C_e} \tag{1}$$

where K_L (L/g) and a_L (L/ μg) are Langmuir constants related to adsorption capacity and free energy of adsorption.

3.1.2. Freundlich isotherm

The Freundlich isotherm describes the non-ideal and reversible adsorption that is not restricted to the formation of a monolayer. This empirical model has been previously applied to multilayer adsorption with non-uniform distribution of adsorption heat and affinities over the heterogeneous surfaces [53]. It is represented by Eq. (2):

$$q_e = a_F C_e^{b_F} \tag{2}$$

where a_F ($\text{L})^{b_F}$ ($\mu\text{g})^{1-b_F} \text{g}^{-1}$ and b_F are the Freundlich adsorption constants and a measure of adsorption intensity, respectively.

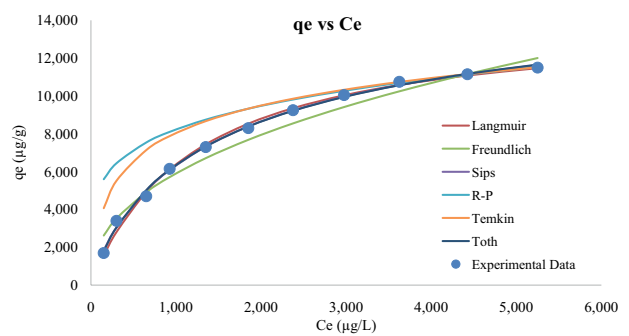


Fig. 2. Equilibrium isotherm modelling results.

3.1.3. Sips (Langmuir–Freundlich) isotherm

The Sips isotherm is a combined form of the Langmuir and Freundlich expressions and has been deduced for predicting the heterogeneous adsorption systems and evading the limitation for the rising adsorbate concentration associated with the Freundlich isotherm model [54]. It is represented by Eq. (3):

$$q_e = \frac{K_{LF} C_e^{n_{LF}}}{1 + (a_{LF} C_e)^{n_{LF}}} \quad (3)$$

where K_{LF} (L/g) and a_{LF} is the Langmuir–Freundlich isotherm constant, and n_{LF} is the isotherm exponent.

3.1.4. Redlich–Peterson isotherm

The Redlich–Peterson isotherm is a hybrid isotherm that has both Langmuir and Freundlich isotherms; the empirical equation has three parameters. The governing model has a linear dependence on concentration in the numerator and an exponential function in the denominator to represent adsorption equilibria over a wide concentration limit. It can be applied either to homogeneous or heterogeneous systems due to its versatility [55]. It is represented by Eq. (4):

$$q_e = \frac{K_{RP} C_e}{1 + a_{RP} C_e^{b_{RP}}} \quad (4)$$

where K_{RP} (L/g) and a_{RP} (L/μg)^b are Redlich–Peterson isotherm constants, and b is the isotherm exponent.

3.1.5. Temkin isotherm

The Temkin isotherm contains a factor that takes into account adsorbent–adsorbate interactions. The model assumes the heat of adsorption of all the molecules in the layer would decrease linearly rather than logarithmic with coverage [56]. It is represented by Eq. (5):

$$q_e = \frac{RT}{b_T} \ln A_T + \left(\frac{RT}{b_T} \right) \ln c_e \quad (5)$$

where A_T (L/g) is the Temkin isotherm equilibrium binding constant, and b_T is the Temkin isotherm constant. R is the gas constant (8.314 kJ/mol K) and T is the temperature at 298 K.

3.1.6. Toth isotherm

The Toth isotherm model is an empirical equation that improves the Langmuir isotherm fittings. It is useful in describing the heterogeneous adsorption systems that satisfy both low- and high-end boundaries of the concentration [57]. It is represented by Eq. (6):

$$q_e = \frac{k_t c_e}{[a_t + c_e^t]^{1/t}} \quad (6)$$

where K_T (μg/g), a_T (μg/L)^t and t characterise the heterogeneity coefficient of the adsorbent.

In order to evaluate the fit of the isotherm equation to the experimental equilibrium data, an error function is required to enable the optimisation procedure. In this study, the sum of squared errors (SSE) was used as the error function to estimate results.

The sum of the squares of the errors method can be represented by the following equation (Eq. (7)):

$$\sum_{n=1}^n (q_{e,cal} - q_{e,meas})^2 \quad (7)$$

where $q_{e,cal}$ is the theoretical adsorbed solid phase concentrations of sorbate on sorbent, which has been calculated from the isotherm equations, and $q_{e,meas}$ is the experimentally determined adsorbed conditions. The SSE is a dimensionless quantity.

The parameters were identified using non-linear regression techniques to minimise the SSE; the results indicated that the Sips (Langmuir–Freundlich) isotherm is the most appropriate model to describe the adsorption of arsenate into nanochitosan over the concentrations studied. The results are shown in Table 3.

3.2. Optimisation to minimise adsorbent mass

The adsorbent system will be designed as a two-stage batch system. In this section of the study, the optimum mass of nanochitosan required for the same is investigated. The process will be designed in such a way that it will have two separate batches of adsorbents with filtration between the stages to enhance the efficiency and minimise the use of adsorbents. Although more stages such as 4 or 5 would enhance the process it is impractical to use more than two stages in industrial applications for batch reactor systems using adsorption treatment.

A schematic flow sheet for a two-equilibrium-stage operation is shown in Fig. 3. The same amount of solution, L_s , is treated in each stage by different amounts of adsorbent, S_{s1} and S_{s2} , in the two stages, respectively. The concentrations of the solution are reduced from C_0 to C_1 and C_1 to C_2 , respectively.

The material balance for stage 1 can be represented by Eq. (8):

$$L_s (C_0 - C_1) = S_{s1} (q_1 - q_0) \quad (8)$$

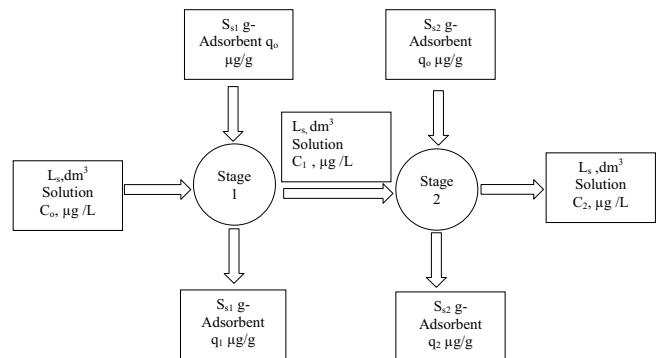


Fig. 3. Schematic figure of a two-stage system.

and for stage 2, the material balance can be represented by Eq. (9):

$$L_s(C_0 - C_1) = S_{s2}(q_2 - q_0) \tag{9}$$

where q_0 is the metal ion concentration of adsorbent entering exchange stages, and q_0 is equal to zero as fresh adsorbent is used in each stage; q_1 and q_2 are the metal ion concentrations of adsorbent leaving the stages 1 and 2, respectively.

As the adsorption isotherm is best represented by the Sips (Langmuir–Freundlich) model, it is used to determine the least amount of mass required in a two-stage adsorber system.

The Sips (Langmuir–Freundlich) isotherm is expressed as:

$$q_e = \frac{K_{LF}C_e^{n_{LF}}}{1 + a_{LF}C_e^{n_{LF}}} \tag{10}$$

Hence, the material balance for stage 1 becomes:

$$\frac{S_{s1}}{L_s} = \frac{C_0 - C_1}{q_1 - q_0} \tag{11}$$

$$\frac{S_{s1}}{L_s} = \frac{(C_0 - C_1)(1 + a_{LF}C_1^{n_{LF}})}{K_{LF}C_1^{n_{LF}}} \tag{12}$$

And for stage 2, it becomes:

$$\frac{S_{s2}}{L_s} = \frac{C_1 - C_2}{q_2 - q_0} \tag{13}$$

$$\frac{S_{s2}}{L_s} = \frac{(C_1 - C_2)(1 + a_{LF}C_2^{n_{LF}})}{K_{LF}C_2^{n_{LF}}} \tag{14}$$

Therefore, the total amount of adsorbent used was:

$$\frac{S_{s1} + S_{s2}}{L_s} = \frac{1}{K_{LF}} \left(\frac{(C_0 - C_1)(1 + a_{LF}C_1^{n_{LF}})}{C_1^{n_{LF}}} + \frac{(C_1 - C_2)(1 + a_{LF}C_2^{n_{LF}})}{C_2^{n_{LF}}} \right) \tag{15}$$

$\frac{d[(S_{s1} + S_{s2})/L_s]}{dC_1}$ was set equal to zero in order to determine the minimum total adsorbent required. Thus, the equation becomes:

$$\frac{1}{K_{LF}} \left[n_{LF} \frac{1}{C_1^{n_{LF}+1}} \left(\frac{C_0}{C_1} + 1 \right) + \frac{1}{C_1^{n_{LF}}} \right] = \frac{1}{K_{LF}C_2^{n_{LF}}} \tag{16}$$

$$\text{Let } X = \left(\frac{C_1}{C_2} \right)^{(b_f)} - b_{(f)} \left(\frac{C_0}{C_1} \right) - 1 + b_f \tag{17}$$

The intermediate concentration, C_1 , was determined by setting the value of X in Eq. (17) to be zero using the solver add-in with Microsoft Excel spreadsheet program.

Thus, the amount of adsorbent required for each stage could be determined by Eqs. (12) and (14).

The mass optimisation modelling is undertaken using the methodology outlined in order to determine the total

minimum mass of adsorbents required in a two-stage batch process. A realistic volume of 1,000 L of water is used in this batch reactor design analysis.

The minimum mass required is calculated for three scenarios:

- $C_2 = 1\% C_0$
- $C_2 = 10 \mu\text{g/L}$ (WHO limit for arsenic in water)
- $C_2 = 5 \mu\text{g/L}$ (estimated future limit for arsenic in water)

The results of the mass modelling indicate that to treat 1,000 L of water with varying initial arsenate concentrations (1,000–12,000 $\mu\text{g/L}$), the amount of nanochitosan required would vary from 1 to 6 kg. In real-life applications, the concentration of arsenate in water would likely be in lower range of concentrations studied hence indicating that the total amount of nanochitosan required to be around 1–3 kg at most. The results are summarised in Fig. 4.

3.3. Batch kinetic studies

The kinetic models of adsorption are used to correlate the adsorbate uptake rate with bulk concentration of adsorbate. It is of paramount importance to study the adsorption kinetics to evaluate the suitability of using the adsorbent for practical demonstrations in water treatment. The kinetics not only provide valuable insights into the reaction mechanisms but will also be used to predict the rate at which the pollutant is removed from the liquid phase in order to design appropriate systems.

3.4. Mechanism

In order to determine the most appropriate model to represent the kinetics involved it is necessary to establish the mechanism of the arsenate removal process from which the order of reaction may be inferred for the adsorption process. The first stage of the mechanism is the protonation of the nanochitosan [47], which is represented by Eq. (18):



The point of zero charge of the nanochitosan was determined to be between $\text{pH}_{\text{pzc}} = 8.0$ and $\text{pH}_{\text{pzc}} = 9.2$. Since the pH

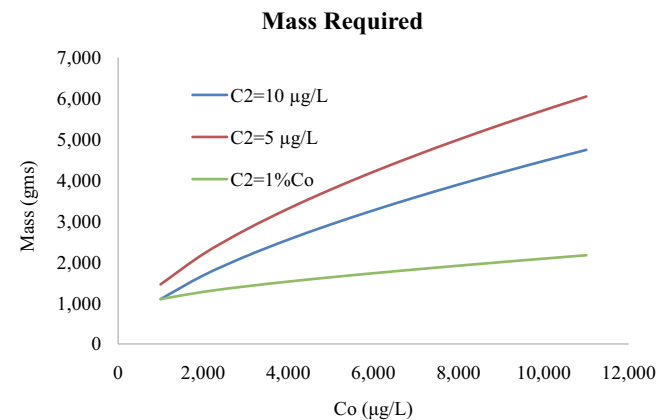


Fig. 4. Mass minimisation results.

of the point of zero charge (pH_{pzc}) is the pH above which the total surface of the particles is negatively charged, the total surface of the nanochitosan is positively charged within the operation range of initial $\text{pH}_i = 3.5$ to the final pH_e values of 5.5–6.5 depending on the initial concentration in this study. The next mechanistic step is to assess how the arsenate species attach to this protonated amino nanochitosan group. The speciation diagram shown in Fig. 5 shows the nature of arsenate species in the solution.

The dominant species of arsenate ions in the final range of pH of 5.5–6.5 is a combination of the monovalent form, H_2AsO_4^- and the divalent form, HAsO_4^{2-} , as shown in Table 4. On this basis the two adsorption arsenate removal equations are represented as follows:

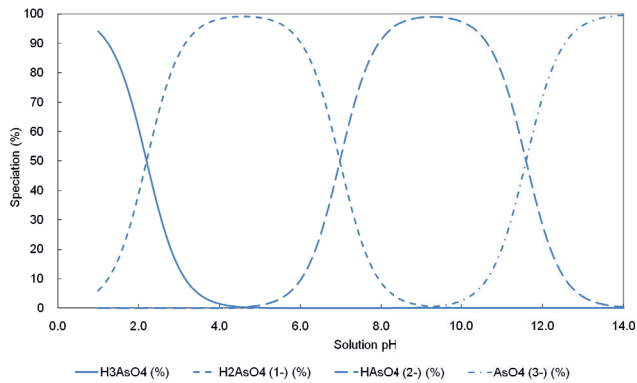
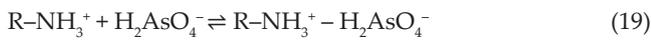


Fig. 5. Arsenate ions, As(V) speciation diagram.

Table 3
Equilibrium isotherm modelling results

Model	Equation	Parameters	Parameter values	SSE results
Langmuir	$q_e = \frac{K_L C_e}{1 + a_L C_e}$	K_L a_L	$K_L = 11.67$ $a_L = 0.00082801$	SSE = 5.49×10^5
Freundlich	$q_e = a_F C_e^{b_F}$	a_F b_F	$a_F = 306.8$ $b_F = 0.428$	SSE = 3.24×10^6
Sips (Langmuir–Freundlich)	$q_e = \frac{K_{LF} C_e^{n_{LF}}}{1 + (a_{LF} C_e)^{n_{LF}}}$	K_{LF} a_{LF} n_{LF}	$K_{LF} = 29.88$ $a_{LF} = 0.00186$ $n_{LF} = 0.8482$	SSE = 3.05×10^5
Redlich–Peterson	$q_e = \frac{K_{RP} C_e}{1 + a_{RP} C_e^{b_{RP}}}$	K_{RP} a_{RP} b_{RP}	$K_{RP} = 2,023$ $a_{RP} = 100.4$ $b_{RP} = 0.7968$	SSE = 3.99×10^7
Temkin	$q_e = \frac{RT}{b_T} \ln A_T + \left(\frac{RT}{b_T} \right) \ln c_e$	A_T b_T	$A_T = 0.04637$ $b_T = 2,095$	SSE = 2.24×10^7
Toth	$q_e = \frac{k_t c_e}{[a_t + c_e^t]^{1/t}}$	k_t a_t t	$k_t = 17,170$ $a_t = 138.1$ $t = 0.7096$	SSE = 3.21×10^5



For the second stage an additional NH_3^+ adsorption site is required to hold the divalent ions, HAsO_4^{2-} . Therefore, the mechanism involves two molecules and three molecules, respectively. A slow desorption of arsenate ions occurs gradually after the point of maximum solid phase concentration. Therefore, in order to identify a kinetic model to describe the adsorption stage, two second-order models are compared in this study namely the pseudo-second-order model and the Elovich model.

3.4.1. Pseudo-second-order model

$$q_t = \frac{q_e^2 k_2 t}{1 + q_e k_2 t} \quad (21)$$

where q_e is the amount of arsenate sorbed at equilibrium ($\mu\text{g g}^{-1}$), and k_2 is the equilibrium rate constant of pseudo-second-order chemical sorption ($\text{g } \mu\text{g}^{-1} \text{ min}^{-1}$) [58] and shown in Eq. (21).

3.4.2. Elovich model

$$q_t = \alpha \ln(a\alpha) + \alpha \ln t \quad (22)$$

where q_t represents the amount of arsenate adsorbed at time t ; a ($\text{g } \mu\text{g}^{-1}$) is the desorption constant and α ($\mu\text{g g}^{-1} \text{ min}^{-1}$) is the initial adsorption rate [59] and shown in Eq. (22).

SSE was used to determine the best-fit model. It is seen that the pseudo-second-order model best fit the data over the range of concentrations studied. The results are shown in Table 5.

It should be stated that in further studies the effect of other anions should be explored since the sequence of anion adsorption shows a marked selectivity which is regulated by its hydrophobic character as predicted by the Hofmeister series [60]. It follows the general role that anions which interact less with water are better extracted from water. Most commercially available anion exchange resins do not have high selectivity to arsenate species over chloride and sulphate.

3.5. Contact time minimisation

In this section, the pseudo-second-order model is used to determine the minimum contact time required for a two-stage process [61,62]. The pseudo-second-order model has been previously used in literature to correlate the kinetic data for arsenate and chitosan adsorption by many researchers in the past [63,64].

By employing the mass balance equation, along with the kinetic model equation, the operating time for each stage can be determined for different amounts of removal.

Fig. 3 is a schematic diagram for a two-stage batch system process. L dm³ wastewater enters stage 1 with S₁ g adsorbent. The concentration of the metal ions is reduced from C₀ to C₁. Then the wastewater is treated in stage 2 with S₂ g adsorbent. The ion concentration is further reduced to C₂.

Generally, the mass balance is shown in Eq. (23):

$$L(C_{n-1} - C_n) = S(q_n - q_0) \tag{23}$$

Table 4
Speciation changes of arsenate ions in aqueous phase upon increasing system pH from monovalent to divalent ions (HAsO₄²⁻)

pH	H ₃ AsO ₄ (%)	H ₂ AsO ₄ ⁻ (%)	HAsO ₄ ²⁻ (%)	AsO ₄ ³⁻ (%)
3.50	4.77	95.20	0.03	2.50 × 10 ⁻¹⁰
4.00	1.56	98.34	0.10	2.59 × 10 ⁻⁹
4.50	0.50	99.17	0.33	2.61 × 10 ⁻⁸
5.00	0.16	98.81	1.03	2.60 × 10 ⁻⁷
5.50	0.05	96.75	3.20	2.54 × 10 ⁻⁶
6.00	0.02	91.08	8.90	2.48 × 10 ⁻⁵
6.50	0.001	74.99	25.0	2.37 × 10 ⁻⁴
6.80	0.00	60.21	39.78	6.31 × 10 ⁻⁴

Table 5
Kinetic modelling results

Parameter	Model Value	Pseudo-second order	Elovich	
		k ₂	α	a
C ₀ (μg/L)	1,000	1.121 × 10 ⁻⁵	197.3	0.00507
C ₀ (μg/L)	2,000	3.988 × 10 ⁻⁶	398.7	0.00251
C ₀ (μg/L)	4,000	2.734 × 10 ⁻⁶	756.05	0.00132
C ₀ (μg/L)	6,000	1.471 × 10 ⁻⁶	1,031	0.000969
C ₀ (μg/L)	8,000	1.378 × 10 ⁻⁶	1,202	0.000832
C ₀ (μg/L)	10,000	1.354 × 10 ⁻⁶	1,320	0.000758
Total	SSE	2.807 × 10 ⁷	8.218 × 10 ⁷	

The pseudo-second-order equation is shown in Eq. (24):

$$\frac{t}{q_1} = \frac{1}{kq_e^2} + \frac{1}{q_e}t \tag{24}$$

By combining Eqs. (23) and (24), the mass balance equation becomes as shown in Eqs. (25) and (26):

$$C_n = C_{n-1} - \frac{Skq_n^2t}{L(1+kq_nt)} \tag{25}$$

$$\sum_{n=1}^n (C_{n-1} - C_n) = \sum_{n=1}^n \frac{Skq_n^2t}{L(1+kq_nt)} \tag{26}$$

The removal of metal ions in each stage, R_n, can be calculated as follows in Eq. (27):

$$R_n = \frac{C_{n-1} - C_n}{C_0} = \frac{Skq_n^2t}{LC_0(1+kq_nt)} \tag{27}$$

The total removal is:

$$\sum_{n=1}^n R_n = \frac{St}{LC_0} \sum_{n=1}^n \frac{kq_n^2}{1+kq_nt} \tag{28}$$

Subsequently, q_e and k are expressed as a function of C₀ when calculated as follows:

$$q_e = A_q C_0^{B_q} \tag{29}$$

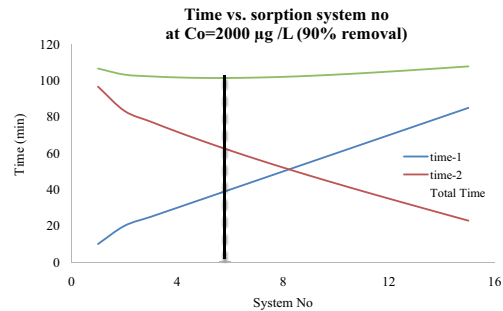


Fig. 6. Contact times study results for 90% arsenate removal at initial concentration (Co) of 2,000 μg/L.

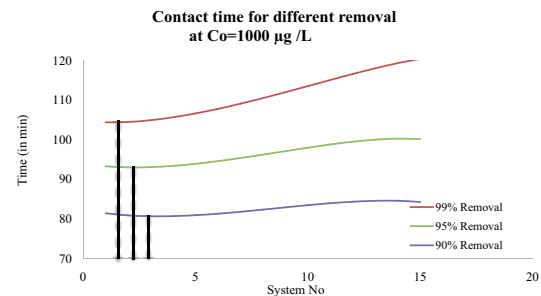


Fig. 7. Summary of contact time results for different removal percentage at Co = 1,000 μg/L.

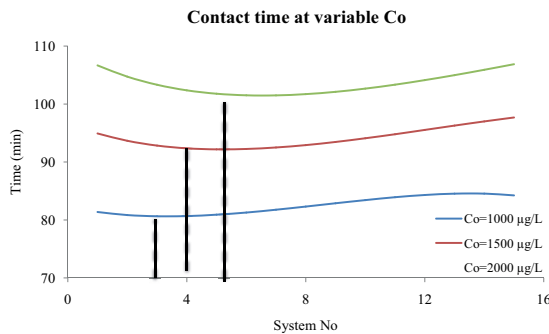


Fig. 8. Summary of the contact time results at different initial concentrations (C_0) at 90% arsenate removal.

$$k = A_k C_0^{B_k} \quad (30)$$

where A_q , B_q , A_k and B_k are constants.

Substitution Eqs. (29) and (30) into Eq. (28):

$$\sum_{n=1}^n R_n = \frac{St}{LC_0} \sum_{n=1}^n \frac{(A_k C_{n-1}^{B_k})(A_q C_{n-1}^{B_q})^2}{1 + (A_k C_{n-1}^{B_k})(A_q C_{n-1}^{B_q})t} \quad (31)$$

By using Eq. (31), the total time for any removal can be calculated.

The parameters A_q , B_q , A_k and B_k are obtained by plotting relevant q_e vs. C_0 and K vs. C_0 graphs.

The contact times for 90%, 95% and 99% of arsenate removal using nanochitosan have been studied to identify the minimum contact times in a two-stage batch process. Arsenate concentrations of 1,000, 1,500 and 2,000 $\mu\text{g/L}$ were used to undertake the contact time modelling. Some of the results obtained are shown in Figs. 6–8, respectively. The minimum contact time is represented in the figures by a dotted line.

The concentration of arsenate studied in the multibatch contact time minimisation studies is likely to be higher than those that would normally exist in contaminated groundwater systems. The results indicate that for the range of concentration studied, the minimum time required in two-stage batch process would normally be around 7–105 min.

4. Conclusion

In this work, the feasibility of the removal of arsenate from water using nanochitosan is studied. The equilibrium and kinetic studies were conducted at a concentration ranging from 1,000 to 12,000 $\mu\text{g/L}$ at a pH of 3.5. The equilibrium data was analysed using various isotherm models, the Sips 3-parameter model demonstrated to provide the best correlation to describe the adsorption of arsenate onto nanochitosan at equilibrium. The mechanism of the arsenate removal process was established to determine the order of reaction for the adsorption process. From the models chosen, it was recognised that the adsorption of arsenate into nanochitosan followed pseudo-second-order adsorption kinetics. The results of the equilibrium and kinetic modelling were used to design an optimised two-stage batch adsorber system for arsenate removal. The minimum mass of nanochitosan adsorbent required in a batch

process was identified for various initial concentrations and provided good results for practical use. Lastly, the contact time to achieve a fixed percentage of arsenate removal using nanochitosan adsorbent was modelled based on a pseudo-second-order equation. This is particularly suitable to design low-cost adsorbent systems where multibatch turn-around time is a critical operational and design benchmark. Moreover, for large-scale operation column studies will be required elution studies will need to be conducted for cost-effective design.

References

- [1] M.A. Khan, Y.S. Ho, Arsenic in drinking water: a review on toxicological effects, mechanism of accumulation and remediation, *Asian J. Chem.*, 23 (2011) 1889–1901.
- [2] I. Ali, H.Y. Aboul-Enein, Speciation of arsenic and chromium metal ions by reversed phase high performance liquid chromatography, *Chemosphere*, 48 (2002) 275–278.
- [3] J.Q. Jiang, S.M. Ashekuzzaman, A. Jiang, S.M. Sharifuzzaman, S.R. Chowdhury, Arsenic contaminated groundwater and its treatment options in Bangladesh, *Int. J. Environ. Res. Public Health*, 10 (2013) 18–46.
- [4] G. Yu, D. Sun, Y. Zheng, Health effects of exposure to natural arsenic in groundwater and coal in China: an overview of occurrence, *Environ. Health Perspect.*, 115 (2007) 636–642.
- [5] World Health Organization, *Guidelines for Drinking Water Quality*, 4th ed., 2011.
- [6] Australian Government, National Health and Medical Research Council, *Australian Drinking Water Guidelines*, National Water Quality Management Strategy, 2011.
- [7] European Commission, *Derogation on the Drinking Water Directive 98/83/EC*, 2010.
- [8] D.N. Mazumder, R. Haque, N. Ghosh, B.K. De, A. Santra, D. Chakraborti, A.H. Smith, Arsenic in drinking water and the prevalence of respiratory effects in West Bengal, India, *Int. J. Epidemiol.*, 29 (2000) 1047–1052.
- [9] Republic of China Environment Protection Administration, Taiwan, 1998.
- [10] P.L. Smedley, D.G. Kinniburgh, Sources and Behaviour of Arsenic in Natural Water, United Nations Synthesis Report on Arsenic in Drinking-Water, Chapter 1, British Geological Survey, Wallingford, Oxon, UK, 2005.
- [11] Y. Glocheux, A.B. Albadarin, C. Mangwandi, E. Stewart, G.M. Walker, Production of porous aluminium and iron sulphated oxyhydroxides using industrial grade coagulants for optimised arsenic removal from groundwater, *J. Ind. Eng. Chem.*, 25 (2015) 56–66.
- [12] D. Mohan, C.U. Pittman Jr., Arsenic removal from water/wastewater using adsorbents – a critical review, *J. Hazard. Mater.*, 142 (2007) 1–53.
- [13] G. Ungureanu, S. Santos, R. Boaventura, C. Botelho, Arsenic and antimony in water and wastewater: overview of removal techniques with special reference to latest advances in adsorption, *J. Environ. Manage.*, 151 (2015) 326–342.
- [14] I. Ali, T.A. Khan, M. Asim, Removal of arsenic from water by electrocoagulation and electro dialysis techniques, *Sep. Purif. Rev.*, 40 (2011) 25–42.
- [15] S. Vasudevan, J. Lakshmi, G. Sozhan, Studies on the removal of arsenate from water through electrocoagulation using direct and alternating current, *Desal. Wat. Treat.*, 48 (2012) 163–173.
- [16] M.R. Awual, M.A. Hossain, M.A. Shenashen, T. Yaita, S. Suzuki, A. Jyo, Evaluating of arsenic(V) removal from water by weak-base anion exchange adsorbents, *Environ. Sci. Pollut. Res.*, 20 (2013) 421–430.
- [17] M.R. Awual, A. Jyo, Rapid column-mode removal of arsenate from water by crosslinked poly(allylamine) resin, *Water Res.*, 43 (2009) 1229–1236.
- [18] M.R. Awual, A. Jyo, S.A. El-Safy, M. Tamada, N. Seko, A weak-base fibrous anion exchanger effective for rapid phosphate removal from water, *J. Hazard. Mater.*, 188 (2011) 164–171.

- [19] M.R. Awual, A. Jyo, Assessing of phosphorus removal by polymeric anion exchangers, *Desalination*, 281 (2011) 111–117.
- [20] S. Vasudevan, J. Lakshmi, G. Sozhan, Studies relating to removal of arsenate by electrochemical coagulation: optimization, kinetics, coagulant characterization, *Sep. Sci. Technol.*, 45 (2010) 1313–1325.
- [21] Y. Yan, C. Chen, Q. Li, X. Sun, L. Wang, Arsenate removal from groundwater by modified alkaline residue, *Desal. Wat. Treat.*, 57 (2016) 20401–20410.
- [22] S. Wang, B. Gao, Y. Li, Enhanced arsenic removal by biochar modified with nickel (Ni) and manganese (Mn) oxyhydroxides, *J. Ind. Eng. Chem.*, 37 (2016) 361–365.
- [23] M.R. Gandhi, S. Vasudevan, A. Shibayama, M. Yamada, Graphene and graphene-based composites: a rising star in water purification – a comprehensive overview, *Chemistry Select*, 1 (2016) 4358–4385.
- [24] S.A. Baig, T. Sheng, Y. Hu, J. Xu, Y. Xu, Arsenic removal from natural water using low cost granulated adsorbents: a review, *Clean*, 43 (2015) 13–26.
- [25] P.K. Dutta, J.V.S. Tripathi, Chitin chitosan: chemistry, properties and applications, *J. Sci. Ind. Res.*, 63 (2004) 20–31.
- [26] T. Yoadsomsuay, N. Grisdanurak, C.-H. Liao, Influence of chitosan on modified nanoscale zero-valent iron for arsenate removal, *Desal. Wat. Treat.*, 57 (2016) 17861–17869.
- [27] S.K. Maji, S.-W. Wang, C.-W. Liu, Arsenate removal from aqueous media on iron-oxide-coated natural rock (IOCNR): a comprehensive batch study, *Desal. Wat. Treat.*, 51 (2013) 7775–7790.
- [28] S. Nigam, K. Gopal, P.S. Vankar, Biosorption of arsenic in drinking water by submerged plant: *Hydrilla verticillata*, *Environ. Sci. Pollut. Res. Int.*, 20 (2013) 1161–1172.
- [29] V.M. Boddu, K. Abburi, J.L. Talbott, E.D. Smith, R. Haasch, Removal of arsenic (III) and arsenic (V) from aqueous medium using chitosan-coated biosorbent, *Water Res.*, 42 (2008) 633–642.
- [30] X. Yu, S. Tong, M. Ge, L. Wu, J. Zuo, C. Cao, W. Song, Synthesis and characterization of multi-amino-functionalized cellulose for arsenic adsorption, *Carbohydr. Polym.*, 92 (2013) 380–387.
- [31] I.A. Oke, N.O. Olarinoye, S.R.A. Adewusi, Adsorption kinetics for arsenic removal from aqueous solutions by untreated powdered eggshell, *Adsorption*, 14 (2008) 73–83.
- [32] M.A. López Leal, R. Cortés Martínez, R. Alfaro Cuevas Villanueva, H.E. Martínez Flores, C. d. J. Cortés Penagos, Arsenate biosorption by iron-modified pine sawdust in batch systems: kinetics and equilibrium studies, *BioResources*, 7 (2012) 1389–1404.
- [33] S. Kamsonlian, S. Suresh, V. Ramanaiah, C.B. Majumder, S. Chand, A. Kumar, Biosorptive behaviour of mango leaf powder and rice husk for arsenic(III) from aqueous solutions, *Int. J. Environ. Sci. Technol.*, 9 (2012) 565–578.
- [34] C. Jeon, Removal of As(V) from aqueous solutions by waste crab shells, *Korean J. Chem. Eng.*, 28 (2011) 813–816.
- [35] S. Deng, Y.P. Ting, Removal of As(V) and As(III) from water with a PEI-modified fungal biomass, *Water Sci. Technol.*, 55 (2007) 177–185.
- [36] R. Jayakumar, M. Prabakaran, S.V. Nair, H. Tamura, Novel chitin and chitosan nanofibers in biomedical applications, *Biotechnol. Adv.*, 28 (2010) 142–150.
- [37] L. Ilium, Chitosan and its use as a pharmaceutical excipient, *Pharm. Res.*, 15 (1998) 1326–1331.
- [38] H.K. No, S.P. Meyers, Application of chitosan for treatment of wastewaters, *Rev. Environ. Contam. Toxicol.*, 163 (2000) 1–27.
- [39] S. Nasirimoghaddam, S. Zeinali, S. Sabbaghi, Chitosan coated magnetic nanoparticles as nano-adsorbent for efficient removal of mercury contents from industrial aqueous and oily samples, *J. Ind. Eng. Chem.*, 27 (2015) 79–87.
- [40] D.-W. Cho, B.-H. Jeon, C.-M. Chon, F.W. Schwartz, Y. Jeong, H. Song, Magnetic chitosan composite for adsorption of cationic and anionic dyes in aqueous solution, *J. Ind. Eng. Chem.*, 28 (2015) 60–66.
- [41] W.-F. Pu, R. Liu, Q. Peng, D.-J. Du, Q.-N. Zhao, Amphiphilically modified chitosan copolymer for enhanced oil recovery in harsh reservoir condition, *J. Ind. Eng. Chem.*, 3 (2016) 216–223.
- [42] L.F. Koong, K.F. Lam, J. Barford, G. McKay, A comparative study on selective adsorption of metal ions using aminated adsorbents, *J. Colloid Interface Sci.*, 395 (2013) 230–240.
- [43] C. Gerente, V.K.C. Lee, P. Le Cloirec, G. McKay, Application of chitosan for the removal of metals from wastewaters by adsorption – mechanisms and models review, *Crit. Rev. Env. Sci. Technol.*, 37 (2007) 41–127.
- [44] Y.C. Wong, Y.S. Szeto, W.H. Cheung, G. McKay, Equilibrium studies for acid dye adsorption onto chitosan, *Langmuir*, 19 (2003) 7888–7894.
- [45] J.C.Y. Ng, W.H. Cheung, G. McKay, Equilibrium studies for the sorption of lead from effluents using chitosan, *Chemosphere*, 52 (2003) 1021–1030.
- [46] J.C.Y. Ng, W.H. Cheung, G. McKay, Equilibrium studies of the sorption of Cu(II) ions onto chitosan, *J. Colloid Interface Sci.*, 255 (2002) 64–74.
- [47] K.C.M. Kwok, L.F. Koong, G. Chen, G. McKay, Mechanism of arsenic removal using chitosan and nanochitosan, *J. Colloid Interface Sci.*, 416 (2014) 1–10.
- [48] J.S. Yamani, S.M. Miller, M.L. Spaulding, J.B. Zimmerman, Enhanced arsenic removal using mixed metal oxide impregnated chitosan beads, *Water Res.*, 46 (2012) 4427–4434.
- [49] Z.G. Hu, J. Zhang, W.L. Chan, Y.S. Szeto, The sorption of acid dye onto chitosan nanoparticles, *Polymer*, 47 (2006) 5838–5842.
- [50] W.H. Cheung, Y.S. Szeto, G. McKay, Enhancing the adsorption capacities of acid dyes by chitosan nano particles, *Bioresour. Technol.*, 100 (2009) 1143–1148.
- [51] K.Y. Foo, B.H. Hameed, Insights into the modeling of adsorption isotherm systems, *Chem. Eng. J.*, 156 (2010) 2–10.
- [52] I. Langmuir, The constitution and fundamental properties of solids and liquids, *J. Am. Chem. Soc.*, 38 (1916) 2221–2295.
- [53] F. Haghseresht, G. Lu, Adsorption characteristics of phenolic compounds onto coal-reject-derived adsorbents, *Energy Fuels*, 12 (1998) 1100–1107.
- [54] R. Sips, Combined form of Langmuir and Freundlich equations, *J. Chem. Phys.*, 16 (1948) 490–495.
- [55] O. Redlich, D.L. Peterson, A useful adsorption isotherm, *J. Phys. Chem.*, 63 (1959) 1024–1026.
- [56] C. Aharoni, M. Ungarish, Kinetics of activated chemisorption. Part 2. Theoretical models, *J. Chem. Soc. Faraday Trans.*, 73 (1977) 456–464.
- [57] J. Toth, State equations of the solid gas interface layer, *Acta Chem. Acad. Hung.*, 69 (1971) 311–317.
- [58] C.A. Zaror, Enhanced oxidation of toxic effluents using simultaneous ozonation and activated carbon treatment, *J. Chem. Technol. Biotechnol.*, 70 (1999) 21–28.
- [59] J. Zeldowitsch, Über den mechanismus der katalytischen oxydation von CO an MnO_2 , *Acta Physicochim.*, URSS, 1 (1934) 364–449.
- [60] F. Hofmeister, Zur Lehre von der Wirkung der Salze: Zweite Mittheilung Arch. Exp. Pathol. Pharmacol., 24 (1888) 247–260.
- [61] Y.S. Ho, G. McKay, A two-stage batch sorption optimized design for dye removal to minimize contact time, *Process. Saf. Environ. Prot.*, 76 (1998) 313–318.
- [62] Y.S. Ho, G. McKay, Pseudo-second order model for sorption processes, *Process Biochem.*, 34 (1999) 451–465.
- [63] M. Annaduzzaman, P. Bhattacharya, M. Ersoz, Z. Lazarova, Characterization of a chitosan biopolymer and arsenate removal for drinking water treatment, *CRCnetBASE/Taylor and Francis*, 2014, pp. 745–747.
- [64] W. Ngah, W.S.A. Kamari, Y.J. Koay, Equilibrium and kinetics studies of adsorption of copper (II) on chitosan and chitosan/PVA beads, *Int. J. Biol. Macromol.*, 34 (2004) 155–161.